Printed ISSN 1330–0016
Online ISSN 1333–9133
CD ISSN 1333–8390
CODEN FIZBE7

ON PRODUCTION OF 'SOFT' PARTICLES IN Au+Au AND Pb+Pb COLLISIONS AT HIGH ENERGIES

A. C. DAS GHOSH[a], GOUTAM SAU[b], S. K. BISWAS[c] and S. BHATTACHARYYA[d,1]

[a]*Department of Microbiology, Surendranath College, Kolkata-700009, India*
E-mail address: dasghosh@yahoo.co.in

[b]*Beramara RamChandrapur High School, South 24-Pgs, 743609(WB), India*
E-mail address: sau_goutam@yahoo.com

[c]*West Kodalia Adarsha Siksha Sadan, New Barrackpore, Kolkata-700131, India*
E-mail address: sunil_biswas2004@yahoo.com

[d]*Physics and Applied Mathematics Unit(PAMU), Indian Statistical Institute, Kolkata - 700108, India E-mail address: bsubrata@www.isical.ac.in*

Received 27 July 2010; Revised manuscript received 11 January 2011
Accepted 19 January 2011 Online 21 May 2011

Production of low-p_T (soft) hadronic particles in high energy collisions constitutes a significant corner of special interests and problems, as the perturbative quantum chromodynamics does not work in this region. We have probed here into the nature of the light particle production in two symmetric nuclear collisions at two neighbouring energies with the help of two non-standard models. The results are found to be in good agreement with data. Despite this, as the models applied here are not intended to provide deep insights into the actual physical processes involved in such collisions, the phenomenological bounds and constraints which cannot be remedied for the present continue to exist.

PACS numbers: 25.75.-q, 13.85.Ni, 13.60.Hb, 13.60.Le UDC 539.126, 539.172

Keywords: relativistic heavy ion collision, inclusive production with identified hadrons, inclusive cross-section, meson production

1. Introduction

Multiple production of hadrons at high energies, named also multiparticle production phenomena, is still not at all a well-understood sector. In general, the largest bulk of the particles produced in nature, called secondaries, is detected to be of the small transverse momenta, though in arranged laboratory collisions at colliders (inclusive of LHC) the particles are, in the main, detected with and reported for large transverse momenta. The theoretical studies based on the standard

[1]Communicating Author

model (SM) of particle interaction are grounded on an artificial division between 'soft' (low-p_T) and 'hard' (large-p_T) regions. The latter, wherein the perturbative techniques are applied, is called perturbative quantum chromodynamics (pQCD), and the former, wherein perturbation theory fails, is termed non-perturbative domain. And most of the particles in nature as well as in laboratory collisions fall under this non-perturbative sector, for whom there is no widely acceptable general theory [1]. Our interest in the present work is focussed on particle production at low-p_T valued Pb+Pb interaction at relatively lower SPS energies. The prime object of this paper is to study the p_T-dependence of the invariant cross-sections for main varieties of hadron secondaries with the help of one or two models which do not typically fall under the standard variety and which will be outlined in the next section. The main species (like kaon, pion, proton) of the secondaries here are pions, kaons and proton-antiproton produced in both lead-lead interactions at $\sqrt{S_{NN}}$=17.3 GeV and $E_{\rm lab}$=20A, 30A, 40A GeV, and Au+Au reactions at RHIC at $\sqrt{S_{NN}}$=19.6 GeV.

In our approach, we would try (i) to demolish the artifact of soft-hard division and try to apply a unified view by treating the production of particles on a uniform footing, (ii) to check whether the outlook of the divide between the exponentialisation and the power-law nature based on the artificial soft-hard boundary is of any real merit or worth, and in probing this point we have been spurred by a very recent report published by Busza [2] with emphasis on the first lesson to be learnt from PHOBOS Collaboration that there is no anomalous production of low-p_T (soft) particles at RHIC, and (iii) to study how the nature of p_T-scaling in the particle production scenario manifests itself in the extreme case of low-p_T and the relatively lower side of the high energy domain i.e., at SPS region.

The work reported here aims at putting a strong question-mark to the time honoured contention of the large bulk of the high-energy physicists that the data on 'soft' collisions could be described by the exponential models; the power laws are applicable for explaining the data on 'hard' collisions. In fact, in this work we have contested this view and have attempted at showing that power laws could be applied almost universally.

The organisation of the work is as follows. In Section 2 we present a brief outline of the very simple theoretical frameworks. The Section 3 embodies the results of the work in graphical plots and tables which show up the used values of the parameters. In Section 4 we have discussed in detail the very minute points that worked in arriving at the desired results and had provided answers to some anticipatory and probable questions from the readers. The last section offers precisely the summary and outlook.

2. Outlines of the theoretical framework

This section is divided into subsections comprising (i) the power-law-based p_T-scaling model (also named the Hagedorn model) and (ii) the combinational approach, both of which are very much in use in recent times by some of us.

2.1. Hagedorn model: Essentially a power law with p_T-scaling

Our objective here is to study the inclusive p_T-spectra of various secondaries of main varieties produced in pp collisions. The kinematics of an inclusive reaction $h_a h_b \longrightarrow hX$ is described by Lorentz invariants. These are e.g. the center-of-mass energy squared $s = (P_a + P_b)^2$, the transverse momentum transverse (squared) $t = (P_h - P_a)^2$ and the missing mass M_X, where M_X is the mass of the undetected components that are produced in the reaction process, denoted by 'X' in $h_a h_b \to hX$. It is common to introduce the dimensionless variables ($u = M_X^2 - s - t$),

$$x_1 = -\frac{u}{s}\,, \quad x_2 = -\frac{t}{s}\,, \tag{1}$$

where s, t and u are called the Mandelstam variables. These variables are related to the rapidity y and radial scaling factor x_R of the observed hadron by

$$y = \frac{1}{2}\log(x_1/x_2)\,, \tag{2}$$

$$x_R = \frac{2|\overrightarrow{p_{cm}}|}{\sqrt{s}} = 1 - \frac{M_X^2}{s} = x_1 + x_2\,. \tag{3}$$

Since most of existing data are at $y = 0$, where $x_R = x_T = 2p_T/\sqrt{s}$ and $|\overrightarrow{p_{cm}}|$ is just the magnitude of the three-momentum in the c.m. system, one often refers to the scaling of the invariant cross section as "x_T scaling". For $y \neq 0$, we find the variable x_R more useful than x_T, since x_R allows a smooth matching of inclusive and exclusive reactions in the limit $x_R \to 1$.

We will assume that at high p_T, the inclusive cross section takes a factorized form. And one such a factorized form was given by Back et al. [3],

$$\frac{\mathrm{d}N}{\mathrm{d}p_T} = \frac{p_T(n-2)(n-1)}{{p_0}^2}\left(1 + \frac{p_T}{p_0}\right)^{-n}, \tag{4}$$

where n and p_0 are adjustable parameters. The exponents n are just numbers. p_0 is to be viewed as an energy-band-dependent critical value of the transverse momentum within the low-p_T limits and is introduced for the sake of making the term within the parenthesis dimensionless, thus lending the expression within the parenthesis a scaling form with p_T/p_0, called p_T-scaling.

With the simplest recasting of form of the above expression (4) and with replacements like p_T=x, p_0=q, $C = a$ normalisation factor, and in the light of the definitions of the inclusive cross-sections, we get the following form as the final working formula

$$z = f(x) = \frac{C}{q^2}\left(1 + \frac{x}{q}\right)^{-n}. \tag{5}$$

2.2. Combinational approach: De-Bhattacharyya model

The combinational approach outlines a method for arriving at the results to be obtained on some observables measured in particle-nucleus or nucleus-nucleus interactions at high energies from those obtained for the basic nucleon-nucleon (or proton-proton) collision. And the results for nucleon-nucleon interactions are based on power-law fits which are assumed to be physically understood somewhat fairly in the light of both thermal model and/or pQCD-related phenomenology. So, this represents essentially a notional combination of power-law model for pp reactions and the introduction of some mass-number-dependent product term signifying the nuclear effects on invariant cross-sections, from which the name 'Combinational Approach' is derived. And this notional combination subsumes the property of factorization which is one of the cardinal principles in the domain of particle physics.

The expression for the transverse momentum-dependence of the inclusive cross-section for secondary particle, Q, produced in nucleus-nucleus (AB) collisions is given by [4] – [7]

$$E\frac{\mathrm{d}^3\sigma}{\mathrm{d}p^3}\Big|_{AB\to QX} \sim (AB)^{f(p_T)} E\frac{\mathrm{d}^3\sigma}{\mathrm{d}p^3}\Big|_{pp\to QX}, \tag{6}$$

where A and B on the right-hand side of the above equation stand for the mass numbers of two colliding nuclei; the term, $E\mathrm{d}^3\sigma/\mathrm{d}p^3\big|_{pp\to QX}$ is the inclusive cross section for production of the same secondary, Q, in pp or $p\overline{p}$ collision at the same center-of-mass (c.m.) energy.

Nature of (p_T)-dependence of the inclusive cross-section term, $E\mathrm{d}^3\sigma/\mathrm{d}p^3\big|_{pp\to QX}$, occurring in Eq. (1) for production of a Q-species in $pp/p\overline{p}$ reactions at high energies, is taken here in the form of a power law as was initially suggested by G. Arnison et al. [8]

$$E\frac{\mathrm{d}^3\sigma}{\mathrm{d}p^3}\Big|_{pp\to QX} \approx C_1\left(1+\frac{p_T}{p_0}\right)^{-n}, \tag{7}$$

where C_1 is the normalization constant, and p_0 and n are two interaction-dependent parameters for which the values are to be obtained by fitting the pp and $p\overline{p}$ data at various energies. Of course, such a power-law form was applied to understand the nature of the transverse momentum spectra of the pion secondaries by some other authors [9] – [12] as well.

Hence, including Eq. (7) and a parametrization for the factor, $f(p_T)$, into Eq. (6), the final working formula is given by [4] – [7]

$$E\frac{\mathrm{d}^3\sigma}{\mathrm{d}p^3}\Big|_{AB\to QX} \approx C(AB)^{(\alpha p_T-\beta p_T^2)}\left(1+\frac{p_T}{p_0}\right)^{-n}, \tag{8}$$

where C, α and β are constants and have to be determined by fitting the measured data on p_T-spectra for production of charged hadrons in nucleus-nucleus collisions at high energies. Some sort of physical interpretations for α and β are given in some of our previous works [5], [6].

A useful way [3], [13] to compare the spectra from nucleus-nucleus collisions to those from nucleon-nucleon collisions is to scale the normalized pp (or $p\overline{p}$) spectrum

(assuming the value of inelastic pp cross-section, $\sigma_{\rm inel}^{pp} \approx 41$ mb) by the number of binary collisions, $\langle N_{\rm coll}\rangle$, corresponding to the centrality cuts applied to the nucleus-nucleus spectra and to construct the ratio. This ratio is called the nuclear modification factor, $R_{\rm AB}$, which is to be expressed in the form

$$R_{\rm AB} = \frac{\dfrac{1}{\langle N_{\rm coll}\rangle} E\dfrac{{\rm d}^3N}{{\rm d}p^3}\Big|_{\rm AB}}{\dfrac{1}{\sigma_{\rm inel}^{PP}} E\dfrac{{\rm d}^3\sigma}{{\rm d}p^3}\Big|_{PP}} \,. \tag{9}$$

It is to be noted here that both the numerator and the denominator of Eq. (9) contain a term of the form $(1 + p_T/p_0)^{-n}$ which gives the p_T-dependence of the hadronic-spectra produced in basic ($pp/p\overline{p}$) collision. And as the other terms, like $\langle N_{\rm coll}\rangle$ and $\sigma_{\rm inel}^{pp}$, are constant for a specific interaction at a definite energy and fixed centrality, we can obtain by combining Eqs. (8) and (9) the final expression for the ratio value in the following form

$$R_{\rm AB} \propto (AB)^{(\alpha p_T - \beta p_T^2)}. \tag{10}$$

The above steps provide the operational aspects of the combinational approach (CA). But this approach outlines a method for arriving at the result to be obtained on some observables measured in particle-nucleus or nucleus-nucleus interactions at high energies from those obtained exclusively for only the basic nucleon-nucleon (or proton-proton) collision. And the results for nucleon-nucleon collisions are based on power-law form (Eq. (7)) which is supposed here to be fairly physically understood in the light of both the thermal model and/or pQCD-related phenomenology. Besides, if the data sets on a specific observable are measured in pp reactions at five or six different high energies at reasonably distant intervals, the pure parameter-effects on p_0 and n could be considerably reduced. Then we may build up a methodology for arriving at p_0 and n values at any other different energy by drawing the graphical plots of p_0 versus $\sqrt{S}$ and n versus $\sqrt{S}$ curves, as was done in some of our previous works [4], [5]. And on this supposition of availability of data in PP reactions at certain intervals of energy values, the number of arbitrary parameters for NA or AA collisions is reduced to only three which offer us quite a handy, useful and economical tool to understand the various aspects of the data characteristics.

The p_0 and n values in Eq. (7) represent the contributions from the basic NN (pp or $p\overline{p}$) collision at a particular energy. The values of p_0 and n are to be obtained from the expressions and plots shown in the work of De et al. [4], [5]. The relevant expressions are

$$p_0(\sqrt{S_{NN}}) = a + \frac{b}{\sqrt{\dfrac{S_{NN}}{{\rm GeV}^2}}\ \ln\sqrt{\dfrac{S_{NN}}{{\rm GeV}^2}}} \,, \tag{11}$$

$$n(\sqrt{S_{NN}}) = a' + \frac{b'}{\ln^2\sqrt{\dfrac{S_{NN}}{{\rm GeV}^2}}} \,. \tag{12}$$

The values of the parameters a, a', b and b' for different secondaries are taken from Ref. [7]. The empirically proposed nature of the plots based on Eq. (11) and Eq. (12) against the data-sets have also been presented for $\pi^{\pm}$, $K^{\pm}$ and $p^{\pm}$ production separately in the following section.

3. Results

In order to attain the comparability of the results obtained at various energies, we have, at the very beginning, converted all relevant energies (with laboratory energies) into the c.m. system. And they have been presented in a tabular form as is given in Table 1. The results of our calculations are presented here in graphical plots and in accompanying tables for the values of the used parameters. In Fig. 1a and Fig. 1b, the differential cross-sections for negative and positive pion, kaon

TABLE 1. Conversion of energy.

Beam Energy	20A GeV	30A GeV	40A GeV
$\sqrt{S_{NN}}$	6.3 GeV	7.6 GeV	8.7 GeV

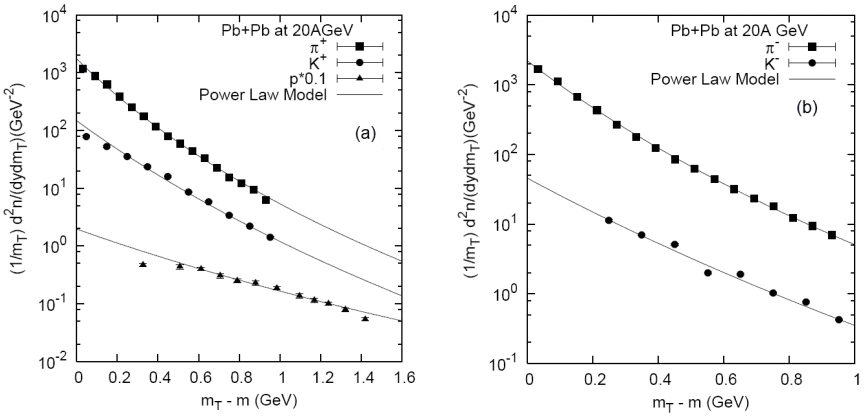

Fig. 1. Transverse mass spectra of π^+, K^+, p (left) and π^-, K^- (right) produced in central Pb+Pb *collisions at* 20A GeV. *The lines are fits of equation of the power-law model. The statistical errors are smaller than the symbol size. Data are taken from Refs. [21] and [22].*

and proton-antiproton production cases in Pb+Pb collisions at SPS energies are reproduced by the used empirical parametrizations given in expressions (4) and (7). The parameter values used to obtain the model-based plots are shown in Table 2. The figures in all cases have been appropriately labeled and the parameters are shown in the tables as mentioned in the text for each case. The data are obtained at such low-p_T values and at the relatively lower side of the high

energy in terms of the m_T values, instead of the p_T values. The relationship between m_T and p_T is generally given by $m_T^2 = m_h^2 + p_T^2$. Within the low-p_T limits

TABLE 2. Numerical values of the fit parameters of power-law equation for Pb+Pb *collisions.*

Beam En.	Prod.	c	q (GeV/c)	n	$\frac{\chi^2}{ndf}$
20A GeV	π^-	43.935 ± 0.015	1.197 ± 0.037	10.010 ± 0.234	0.612/7
20A GeV	π^+	38.950 ± 0.233	1.178 ± 0.087	9.410 ± 0.531	2.628/6
20A GeV	K^-	1.690 ± 0.013	2.404 ± 0.014	14.003 ± 0.054	0.806/4
20A GeV	K^+	5.515 ± 0.136	2.001 ± 0.022	11.888 ± 0.180	4.894/4
20A GeV	p	3.568 ± 0.062	2.757 ± 0.138	8.006 ± 0.352	0.904/4

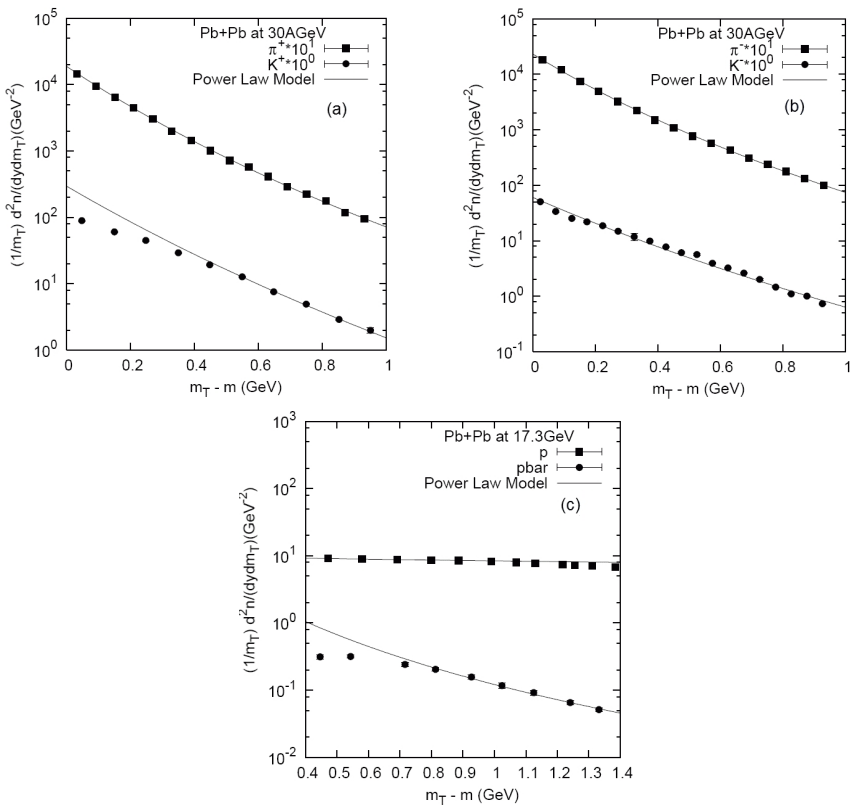

Fig. 2. Transverse mass spectra of π^+, K^+ (upper left), π^-, K^- (upper right) and p, $\overline{p}$ (lower) produced in central Pb+Pb *collisions at* 30A GeV *and 17.3* GeV. *The lines are fits of equation of the power-law model. The statistical errors are smaller than the symbol size. Data are taken from Refs. [21] and [23].*

TABLE 3. Numerical values of the fit parameters of power-law equation for Pb+Pb *collisions.*

Beam En.	Prod.	c	q (GeV/c)	n	$\frac{\chi^2}{ndf}$
30A GeV	π^-	52.202 ± 0.307	1.158 ± 0.073	9.232 ± 0.438	1.158/5
30A GeV	π^+	47.041 ± 0.637	1.344 ± 0.211	10.026 ± 1.166	5.790/8
30A GeV	K^-	2.551 ± 0.040	2.001 ± 0.021	11.240 ± 0.115	3.519/3
30A GeV	K^+	8.962 ± 0.341	1.999 ± 0.017	12.986 ± 0.293	3.697/4
17.3 GeV	p	15027.3 ± 34.99	2.047 ± 0.0001	8.504 ± 0.011	1.252/4
17.3 GeV	$\overline{p}$	0.450 ± 0.042	0.439 ± 0.049	3.999 ± 0.037	1.338/5

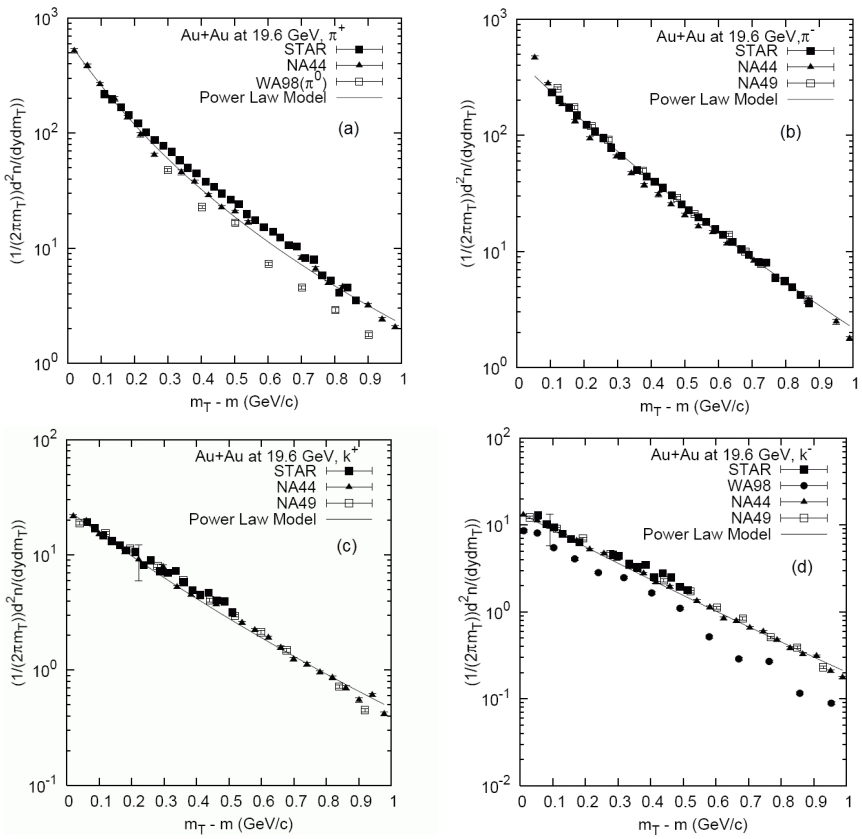

Fig. 3. Transverse mass spectra of π^+ (upper left), π^- (upper right) and K^+ (lower left), K^- (lower right) from the STAR experiment at 19.6 GeV *in* Au+Au *collisions and the results of SPS experiments NA44, NA49, WA98 at 17.3* GeV *in* Pb+Pb *collisions. The line is fit of equation of the power-law model with the STAR and SPS experiment. Data are taken from Ref. [24] and all errors are only statistical.*

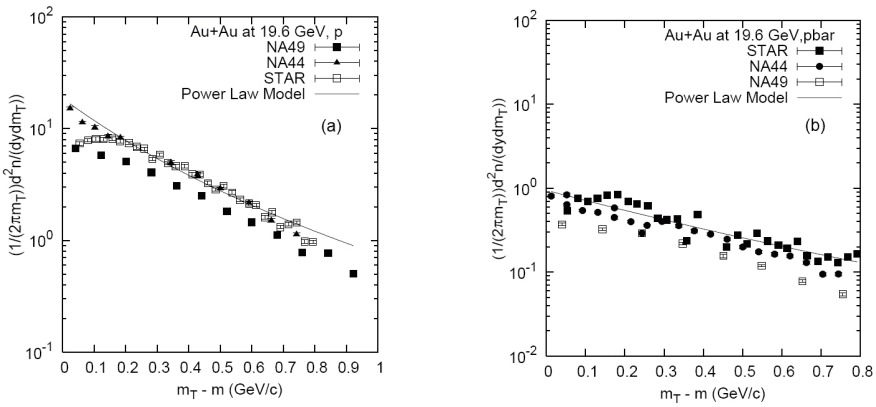

Fig. 4. Transverse mass spectra of p (left) and $\overline{p}$ (right) from the STAR experiment at 19.6 GeV *in* Au+Au *collisions and the results of the SPS experiments NA44, NA49, WA98 at 17.3* GeV *in* Pb+Pb *collisions. The line is a fit of equation of the power-law model with the STAR and SPS experiment. The data are taken from Ref. [24]. The statistical errors are smaller than the symbol size.*

TABLE 4. Numerical values of the fit parameters for pion, kaon, proton and antiproton using power-law model for Au+Au *collisions at 19.6* GeV.

Beam En.	Prod.	c	q (GeV/c)	n	$\frac{\chi^2}{ndf}$
19.6 GeV	π^+	12.588 ± 0.183	0.559 ± 0.061	5.547 ± 0.358	6.518/7
19.6 GeV	π^-	13.443 ± 0.089	2.001 ± 0.011	13.192 ± 0.065	27.759/29
19.6 GeV	K^+	1.455 ± 0.017	2.002 ± 0.256	9.803 ± 0.109	13.526/11
19.6 GeV	K^-	0.742 ± 0.007	6.640 ± 0.038	29.998 ± 0.050	27.027/18
19.6 GeV	p	1.995 ± 0.027	0.887 ± 0.103	4.257 ± 0.233	18.933/11
19.6GeV	$\overline{p}$	0.188 ± 0.005	2.440 ± 0.057	7.001 ± 0.044	2.741/06

and for the low-mass particles ($m_h \ll p_T$) produced in any high energy collisions, $m_T \approx p_T$. As the measured data are obtained and exhibited with m_T on the abscissa, we choose to retain them intact; the ordinate-observable, too, is kept thus undisturbed. The plots in Fig. 2a and Fig. 2b are for positive and negative pion, positive and negative kaon in Pb+Pb collisions at 30A GeV and the corresponding parameters are depicted in Table 3. The plots presented in Fig. 2c for proton-antiproton production in lead-lead interaction at SPS energies, specifically at 17.3 GeV, and the corresponding parameters are depicted in Table 3. The graphs in Fig. 3 and Fig. 4 present the results for the secondaries $\pi^{\pm}$, $K^{\pm}$ and proton-antiproton produced in the Au+Au collisions at 19.6 GeV. The used parameter values for these two figures are given in Table 4. The rest of the figures demon-

strated in the Fig. 5, Fig. 6, Fig. 8 and Fig. 9 are for collisions as labelled and are based on the De-Bhattacharyya model for the major varieties of hadronic secondaries produced at four very close energies as mentioned in each of the figures

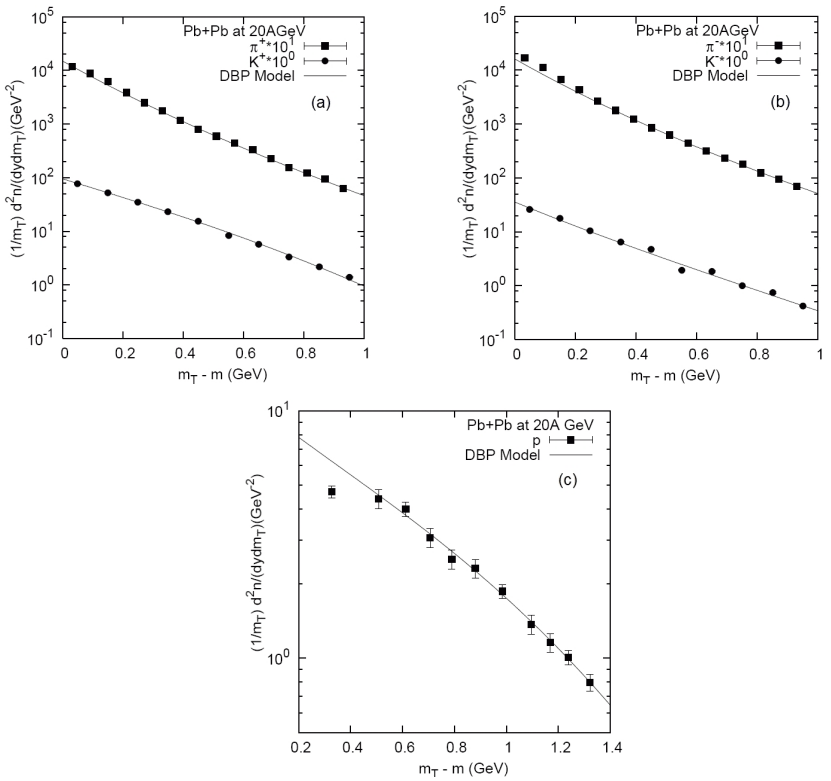

Fig. 5. Transverse mass spectra of π^+, K^+ (upper left), π^-, K^- (upper right) and p (lower) produced in central Pb+Pb *collisions at* 20A GeV. *The lines are fits of equation of the DBP model. The statistical errors are smaller than the symbols. Data are taken from Refs. [21] and [22].*

TABLE 5. Numerical values of the fit parameters of DBP equation for Pb+Pb *collisions.*

Beam En.	Prod.	c	α	β	$\frac{\chi^2}{ndf}$
20A GeV	π^-	1608.85 ± 18.320	0.020 ± 0.008	0.004 ± 0.010	20.330/12
20A GeV	π^+	1492.27 ± 61.830	0.031 ± 0.017	0.018 ± 0.018	19.790/10
20A GeV	K^-	35.667 ± 0.151	0.202 ± 0.010	0.083 ± 0.010	9.847/4
20A GeV	K^+	94.412 ± 2.063	0.334 ± 0.013	0.211 ± 0.014	2.456/3
20A GeV	p	11.309 ± 4.938	0.522 ± 0.106	0.142 ± 0.066	2.148/4

separately. The parameter values used to obtain the nature of the fits are shown in Tables 5, 6 and 9. The graphs plotted in Fig. 7 are based on both the power-

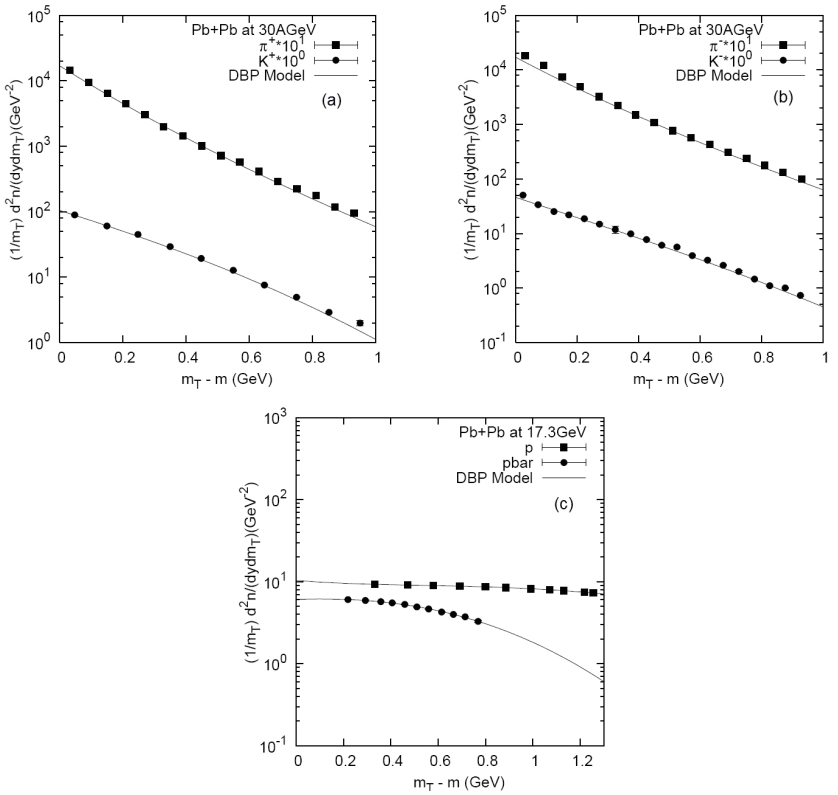

Fig. 6. Transverse mass spectra of π^+, K^+ (upper left), π^-, K^- (upper right) and p, $\overline{p}$ (lower) produced in central Pb+Pb *collisions at* 30A GeV *and 17.3* GeV. *The lines are fits of equation of the DBP model. The statistical errors are smaller than the symbol size. The data are taken from Refs. [21] and [23].*

TABLE 6. Numerical values of the fit parameters of DBP equation for Pb+Pb *collisions.*

Beam En.	Prod.	c	α	β	$\frac{\chi^2}{ndf}$
30A GeV	π^-	1707.12 ± 18.260	0.059 ± 0.007	0.029 ± 0.009	21.159/12
30A GeV	π^+	1697.79 ± 27.510	0.050 ± 0.002	0.026 ± 0.004	24.543/15
30A GeV	K^-	45.951 ± 1.407	0.302 ± 0.013	0.181 ± 0.013	15.312/12
30A GeV	K^+	104.667 ± 2.330	0.373 ± 0.011	0.244 ± 0.012	5.078/5
17.3 GeV	p	10.352 ± 0.070	0.654 ± 0.002	0.121 ± 0.001	0.635/8
17.3 GeV	$\overline{p}$	6.084 ± 0.121	0.723 ± 0.009	0.281 ± 0.009	2.259/8

law model and DBP model, respectively, at 40A GeV in Pb+Pb collisions. The parameter values obviously remain the same as given in Table 7 and Table 8.

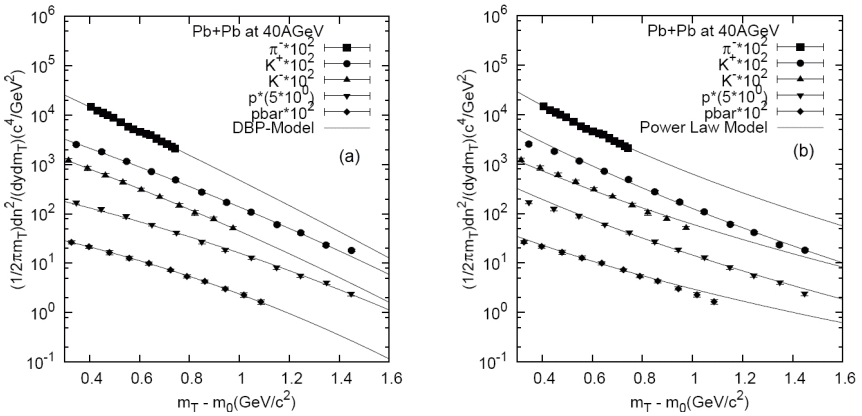

Fig. 7. Transverse mass spectra of K^+, K^-, p, $\overline{p}$ and π^- produced in central Pb+Pb *collisions at* 40A GeV. *The lines are fits of equation of the DBP model [left figure] and the power-law model [right figure]. The statistical errors are smaller than the symbol size. Data are taken from Ref. [22].*

TABLE 7. Numerical values of the fit parameters for negative pion, positive and negative kaon, proton and antiproton using DBP model for Pb+Pb *collisions at* 40A GeV.

Beam En.	Prod.	c	α	β	$\frac{\chi^2}{ndf}$
40A GeV	π^-	1302.44 ± 9.467	0.079 ± 0.008	0.065 ± 0.012	0.109/15
40A GeV	K^+	108.27 ± 0.428	0.220 ± 0.002	0.090 ± 0.003	0.328/13
40A GeV	K^-	44.963 ± 0.323	0.200 ± 0.005	0.093 ± 0.006	0.099/13
40A GeV	p	80.879 ± 1.260	0.346 ± 0.007	0.109 ± 0.006	0.638/14
40A GeV	$\overline{p}$	0.599 ± 0.004	0.382 ± 0.005	0.145 ± 0.006	0.129/14

The graphs plotted in Fig. 10a and Fig. 11a are based on the power-law model and the DBP model, respectively; they represent the fits to the invariant p_T-spectra for production of the main varieties of secondaries in 19.6 GeV Au+Au collisions at mid-rapidity and in the range of 0 – 10% centrality which covers the highest centrality region of nuclear collisions. The parameter values used are given in Table 10 and Table 11. The rest of the plots in Fig. 10 and Fig. 11 are for the nature of the charge-ratio behaviour for the specific variety of the secondary particles. Figure 10b, Fig. 10c and Fig. 10d are drawn on the basis of the power-law model; and the plots shown in Fig. 11b, Fig. 11c and Fig. 11d are on the basis of the DBP model for the same set of charge-ratios.

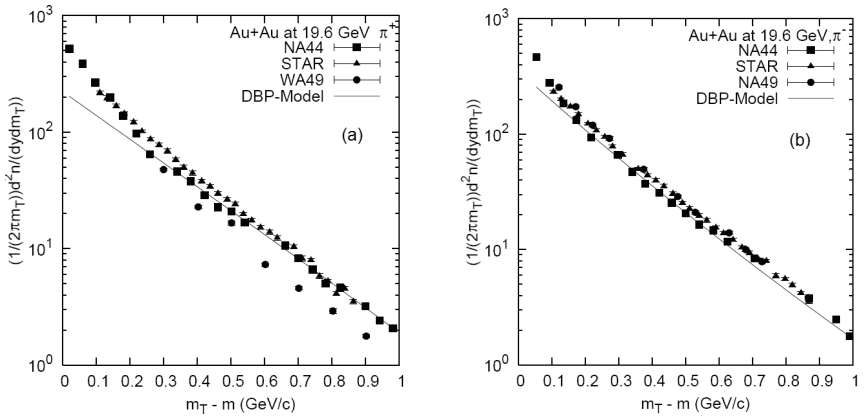

Fig. 8. The transverse mass spectra of π^+ (left) and π^- (right) from the STAR experiment at 19.6 GeV *in* Au+Au *collisions and the results of SPS experiments NA44, NA49, WA98 at 17.3* GeV *in* Pb+Pb *collisions. The line is a fit of equation of the power-law model with the STAR and SPS experiment. The data are taken from Ref. [24]. The statistical errors are smaller than the symbol size.*

TABLE 8. Numerical values of the fit parameters for negative pion, positive and negative kaon, proton and antiproton using power-law model for Pb+Pb *collisions at* 40A GeV.

Beam En.	Prod.	c	q (GeV/c)	n	$\frac{\chi^2}{ndf}$
40A GeV	π^-	54.328 ± 1.296	1.198 ± 0.022	10.003 ± 0.042	0.103/15
40A GeV	K^+	9.176 ± 0.166	1.999 ± 0.007	13.856 ± 0.132	0.617/07
40A GeV	K^-	2.429 ± 0.067	1.734 ± 0.048	10.031 ± 0.210	1.114/11
40A GeV	p	12.827 ± 0.589	1.629 ± 0.043	10.002 ± 0.070	0.433/08
40A GeV	$\overline{p}$	0.078 ± 0.002	1.382 ± 0.054	7.022 ± 0.178	0.800/08

At last, even on the basis of a very few four close-ranging energies and on an approximation that the measured data-values on Pb+Pb and Au+Au at the neighboring would not differ too much, we tried to check here the merits of the phenomenological energy-dependences proposed by us in Eqs. (11) and (12) of the two key parameters, viz, p_0 and n. In Figs. 12 to 14, we plotted the parameter values p_0 along the Y-axis with the energy-values as the corresponding X-axis. The dotted curves in all these figures depict the nature of the parameters obtained by the proposed empirical expressions represented by Eqs. (11) and (12). The phenomenologically formulated expressions reproduce fairly well the nature of fit-values used for the two parameters. Despite the limitations pointed here and before, and by some others, the agreements are modestly encouraging.

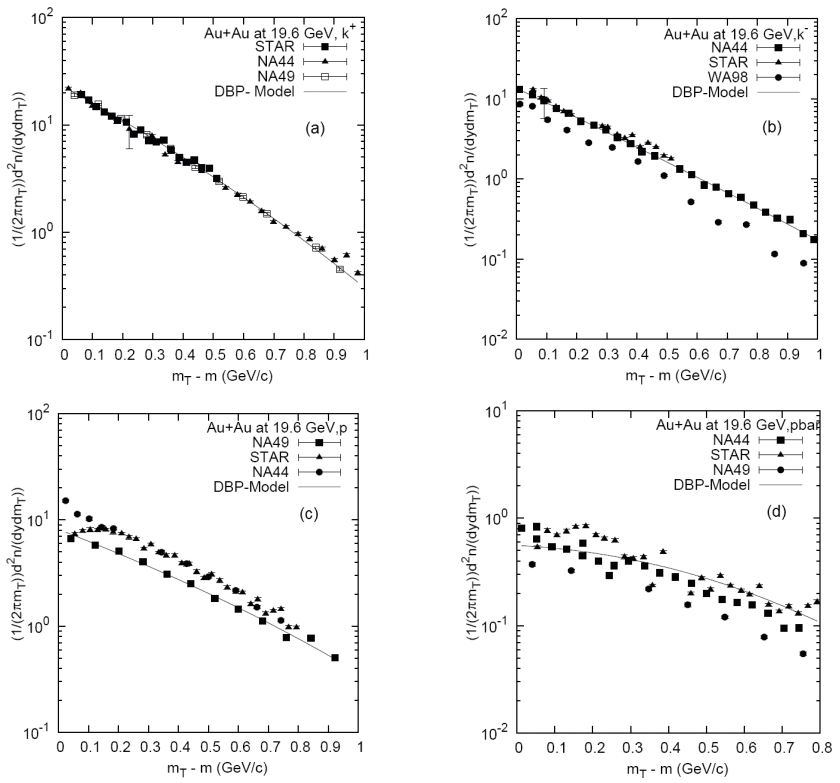

Fig. 9. Transverse mass spectra of K^+ (upper left), K^- (upper right), p (lower left) and $\overline{p}$ (lower right) from the STAR experiment at 19.6 GeV *in* Au+Au *collisions and the results of the SPS experiments NA44, NA49, WA98 at 17.3* GeV *in* Pb+Pb *collisions. The line is fit of equation of the power-law model with the STAR and SPS experiment. The data are taken from Ref. [24]. All errors are only statistical.*

TABLE 9. Numerical values of the fit parameters for pion, kaon, proton and antiproton using DBP model for Au+Au *collisions at 19.6* GeV.

Beam En.	Prod.	c	α	β	$\frac{\chi^2}{ndf}$
19.6 GeV	π^+	223.493 ± 28.050	0.239 ± 0.037	0.100 ± 0.027	4.202/6
19.6 GeV	π^-	352.948 ± 12.490	0.113 ± 0.006	0.029 ± 0.002	3.292/5
19.6 GeV	K^+	22.951 ± 0.709	0.350 ± 0.014	0.168 ± 0.015	9.672/8
19.6 GeV	K^-	13.611 ± 0.041	0.287 ± 0.005	0.110 ± 0.006	19.681/19
19.6 GeV	p	7.030 ± 0.044	0.648 ± 0.004	0.168 ± 0.006	15.994/14
19.6 GeV	$\overline{p}$	0.557 ± 0.021	0.649 ± 0.024	0.297 ± 0.032	4.117/4

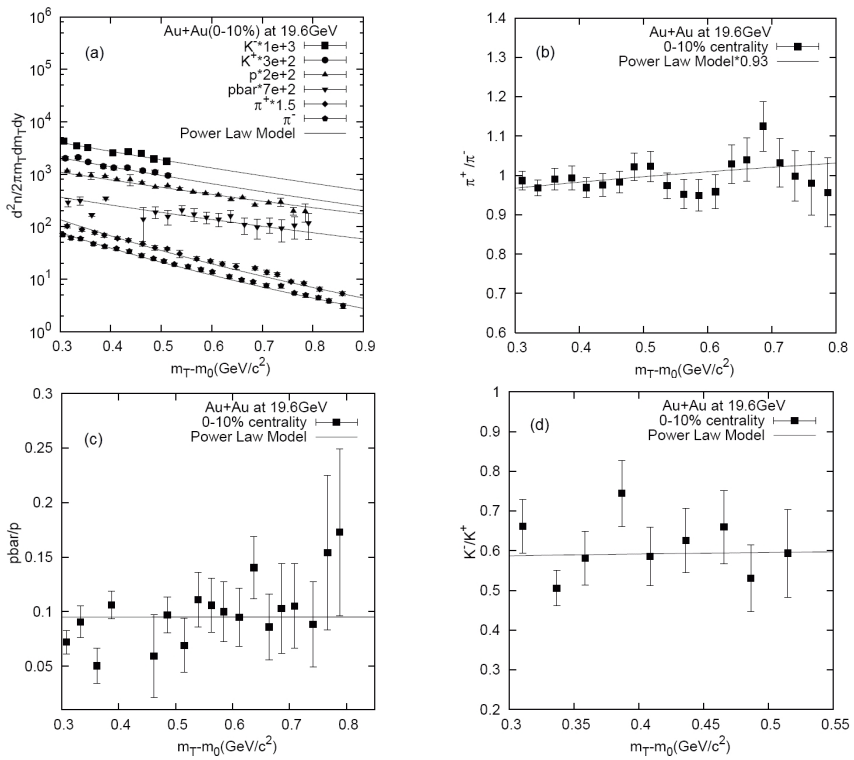

Fig. 10. (a) Transverse mass spectra of identified hadrons measured at midrapidity ($|y| < 0.1$). The results at $\sqrt{s_{NN}}$=19.6 GeV for the production of π^+, π^-, p, $\overline{p}$, K^+ and K^- for 0–10% centrality in Au+Au *collisions. The solid curves provide the power-law-model based results. The data are taken from Ref. [25]; (b),(c),(d) π^-/π^+, $\overline{p}/p$ and K^-/K^+ ratios vs. $m_T - m_0$ for 0–10% centrality in* Au+Au *collisions at $\sqrt{s_{NN}}$=19.6 GeV ($-0.1 < y < 0.1$). The solid curves provide the power-law-model based results. The data are taken from Ref. [25]. All errors are only statistical.*

TABLE 10. Numerical values of the fit parameters for pion, kaon, proton and antiproton using Power Law Model for Au+Au *collisions at 19.6* GeV *for 0–10% centrality.*

Beam En.	Prod.	c	q (GeV/c)	n	$\frac{\chi^2}{ndf}$
19.6 GeV	π^+	18.522 ± 0.520	0.592 ± 0.019	6.689 ± 0.156	20.538/13
19.6 GeV	π^-	15.410 ± 0.302	0.658 ± 0.026	6.834 ± 0.216	13.235/13
19.6 GeV	K^+	1.686 ± 0.028	1.833 ± 0.070	8.648 ± 0.234	0.841/19
19.6 GeV	K^-	0.999 ± 0.039	1.999 ± 0.032	9.123 ± 0.264	0.700/12
19.6 GeV	p	1.672 ± 0.016	1.567 ± 0.025	6.587 ± 0.066	10.212/16
19.6GeV	$\overline{p}$	0.159 ± 0.002	1.568 ± 0.018	6.587 ± 0.052	8.980/21

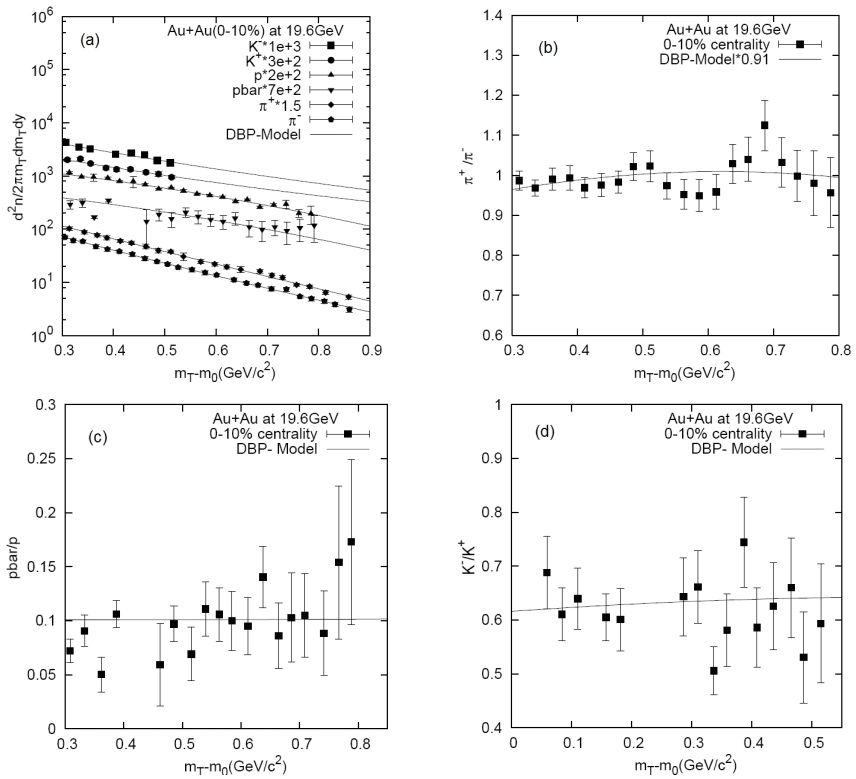

Fig. 11. (a) Transverse mass spectra of identified hadrons measured at midrapidity ($|y| < 0.1$). *The results at* $\sqrt{s_{NN}}$=*19.6* GeV *for the production of* π^+, π^-, p, $\overline{p}$, K^+ *and* K^- *for 0–10% centrality in* Au+Au *collisions. The solid curves provide the DBP model based results. The data are taken from Ref. [25]; (b),(c),(d)* π^-/π^+, $\overline{p}/p$ *and* K^-/K^+ *ratios vs.* $m_T - m_0$ *for 0–10% centrality in* Au+Au *collisions at* $\sqrt{s_{NN}}$=*19.6* GeV ($-0.1 < y < 0.1$). *The solid curves provide the DBP-model-based results. Data are taken from Ref. [25] and all errors are only statistical.*

TABLE 11. Numerical values of the fit parameters for pion, kaon, proton and antiproton using DBP Model for Au+Au *collisions at 19.6* GeV *for 0–10% centrality.*

Beam En.	Prod.	c	α	β	$\frac{\chi^2}{ndf}$
19.6 GeV	π^+	435.425 ± 20.210	0.353 ± 0.021	0.085 ± 0.022	11.887/26
19.6 GeV	π^-	465.221 ± 16.760	0.301 ± 0.016	0.043 ± 0.016	6.918/29
19.6 GeV	K^+	24.176 ± 0.328	0.484 ± 0.004	0.009 ± 0.001	10.611/19
19.6 GeV	K^-	14.898 ± 0.274	0.469 ± 0.005	0.018 ± 0.012	8.199/13
19.6 GeV	p	11.273 ± 0.103	0.731 ± 0.002	0.271 ± 0.003	14.043/21
19.6 GeV	$\overline{p}$	1.139 ± 0.018	0.730 ± 0.006	0.269 ± 0.015	12.847/21

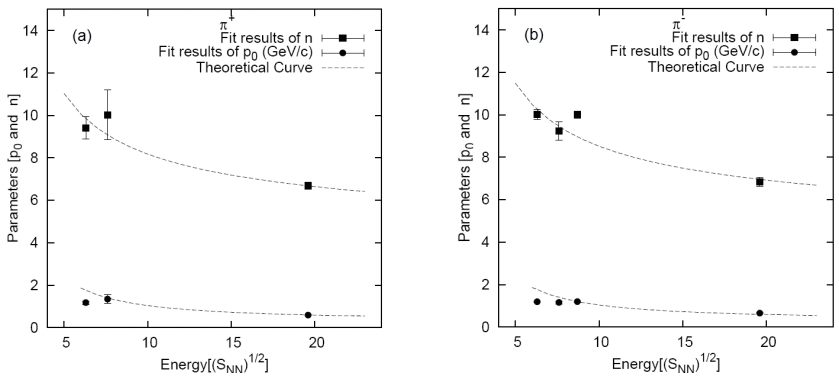

Fig. 12. Values of p_0 and n as a function of c.m. energy $\sqrt{S_{NN}}$. The dotted curves are drawn for π^+ and π^- on the basis of Eqs. (11) and (12).

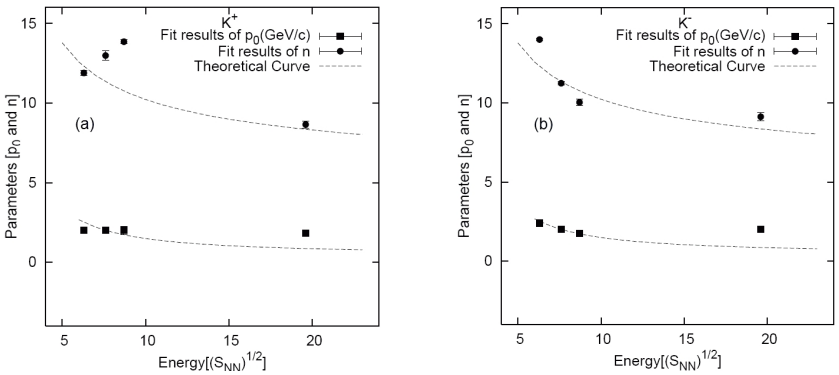

Fig. 13. Values of p_0 and n as a function of c.m. energy $\sqrt{S_{NN}}$. The dotted curves are drawn for K^+ and K^- on the basis of Eqs. (11) and (12).

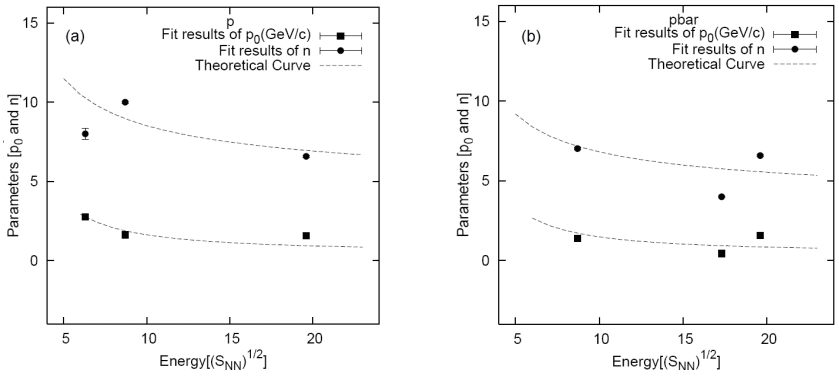

Fig. 14. Values of p_0 and n as a function of c.m. energy $\sqrt{S_{NN}}$. The dotted curves are drawn for p and $\overline{p}$ on the basis of Eqs. (11) and (12).

4. General discussion and some specific points

By all indications, the results manifested in the measured data on the specific observables chosen here are broadly consistent with both approaches applied in this work. This is modestly true of even the nature of charge-ratios which provide virtually a cross-check of the models utilised here. Of course, at this point let us make some comments on our model-based plots, especially the plots on the charge-ratios. This is not very surprising in the sense that the De-Bhattacharyya phenomenology (DBP) through a parametrization is also essentially a power-law model with a bare A-dependence, while in the pure power-law model any of the chosen parameters absorb the nuclear-dependence. Still, the DBP-model inducts some physical postulates which are as follows: (i) It is assumed that the inclusive cross section of any particle in a nucleus-nucleus (AB) collision can be obtained from the production of the same in nucleon-nucleon collisions by multiplying by a product of the atomic numbers of each of the colliding nuclei raised to a particular function, $\epsilon(y, p_T)$, which at first is unspecified (Eq. 6), (ii) Second, we have accepted that factorization [14] of the function $\epsilon(y, p_T)$ is $\epsilon(y, p_T) = f(y)g(p_T)$ which helps us to perform the integral over p_T in a relatively simpler manner, (iii) Finally, we have based on the ansatz that the function $f(y)$ can be modeled by a quadratic function with the parameters α and β (Eq. 10). They are to be tested in the high-energy experiments of the future accelerator generations. Besides, the present DBP-based approach is to deal with the data advances in a systematic methodical approach in which the main parameters could be determined and ascertained, if and only if measured laboratory data of higher accuracy and precision are available at different energies in regular and successive intervals. So, the lack of predictivity of the used two models is caused only by the circumstances, i.e. the lack of measured data at the successive and needed intervals, the problem can be remedied by supplying the necessary and reliable data from the arranged laboratory experiments at high-to-very high energies. However, the problem of constraining the parameters still remains. The other observations are: as is expected for two symmetric collisions of neighbouring values of mass numbers at very close energies, the measured data do not reveal any significant differences with respect to the observables chosen by the experimental groups. This work demonstrates somewhat convincingly that the power-law models can easily take care of data even for very low-p_T (soft) collisions. So the notion of compartmentalisation between the possible applicability of the power-law models and of the exponential models is only superficial. Besides, the power-law models, which establish them as more general ones, obtain a clear edge over the exponential models. Reliable data on various other related observables are necessary for definitive final conclusions. By all indications, the experimentally observed nature of p_T-scaling is found to remain valid even in the studied low-p_T range of this paper. The deeper physical implications of this work have implicity been pointed out in the last two paragraphs of the Section 1 of this work, wherein we made very clear and categorical statements on our intentions, purposes and the prime objectives. So, in order to avoid repetition, we refrain ourselves here very carefully from commiting a rehash of the same. However, let us now try to pinpoint below some physical points and considerations which provide the necessary

underpinning of the power-law models.

The wide and near successful applications of the various forms of power laws have, by now, grown almost universal in almost all branches of physics as well as in other branches of science. Speaking in the most general and scientific terms, the processes which are complex, violent and dissipative contributing to the non-equilibrium phenomena do generally subscribe to the power laws. The used power law behaviors are commonly believed to be the "manifestations of the dynamics of complex systems whose striking feature is of showing universal laws characterized by exponents in scale invariant distributions that happen to be basically independent of the details in the microscopic dynamics [15]". Now let us revert from the general to the particular case(s) of high-energy particle-particle, particle-nucleus or nucleus-nucleus collisions. For purely hadronic, hadronuclear or nuclear interactions, one of the basic features is: irrespective of the initial state, agitations caused by the impinging projectile (be it a parton or a particle/nucleon) generate system effects of producing avalanches of new kind of partons [called quark(s)/gluon(s)/any other(s)] which form an open dissipative system. The avalanches caused by the production of excessive number of new partons give rise to the well-known phenomenon of jettiness of particle production processes and of cascadisation of the particle production processes leading to the fractality as was shown in the paper by Sarcevic [16]. These cascades are self-organizing, self-similar and do just have the fractal behavior. Driven by the physical impacts of these well-established facts, in the high-energy collision processes do crop up the several power laws. And how such power laws do evolve from exponential origins or roots is taken care of by the induction of the Tsallis entropy [17] and a generalisation of Gibbs-Boltzmann statistics for long-range and multifractal processes. Following Sarcevic [16], the relationship between/among cascadisation, self-similarity and fractality is/was evinced in the paper [18] by a set of the present authors. In this paper we have, once more, tried to examine the worth and utility of such power laws as have been advocated here.

In the data-plots of Fig. 3a, we observe some differences between the trends of WA98 data and the other. But it is to be noted that the data in WA98 experiment are for the observation of neutral pions, whereas our plot is intended to be one of the charged varieties of pions, e.g., π^+ detected at the experimental energy 17.3 GeV in c.m. system; besides, the STAR data were measured at 19.6 GeV (c.m.). Apart from this, in the WA98 experiment the observable along the Y-axis was just $E\mathrm{d}^3\sigma/\mathrm{d}p^3$, whereas for the others the Y-axis was described to be $\frac{1}{2\pi}\mathrm{d}^2n/(m_T\mathrm{d}m_T\mathrm{d}y)$. The data from WA98 took up values of $m_T - m_0$ from 1 to 4 GeV/c. But all other plots were limited to just $m_T - m_0$=1 GeV/c. So there are a host of factors of differences between WA98 data and the rest. The differences in the magnitudes of the π^+ plots in the invariant cross section between various data sets might be a cumulative effect of all the above-mentioned factors.

Quite spectacularly, in Fig. 3d for the production of K^-, the differences between the data-points measured by WA98 and the rest are surely non-negligible. So the existence of a discrepancy to a certain degree cannot be denied.

However, one must note that the observable plotted as ordinate in the WA98 experimental data is a bit different from the others, where does occur a term denoted

by N_{evt} related with both statistical and systematic uncertainties, though the uncertainties in all other cases (i.e., for non-WA98) the errors are only statistical. Our guess is: the twin factors of systematic uncertainties and the separate y-observable [in the WA98] along the ordinate are responsible for introducing such differences as are shown in data-plot of Fig. 3d. The reason(s) might also be something else.

We observe that the data points on invariant cross-sections for production of protons show relatively much slower fall with m_T (p_T) than the other prime varieties of hadrons. Thus one might have doubts on the accuracy of data-measurements and recordings for protons. If this is too unlikely to be the case, we guess that in the detection/measurement process the part of the 'leading' protons has disguised themselves and appeared as the product proton-particles enhancing protonic invariant cross-section for which the fall in the invariant cross-section with m_T is much less. This explanation is certainly just tentative.

In the end, one more comment is in order. Quite knowingly, we used here the usual binned χ^2-method with the attending limitations of this approach to check the goodness-of-fit of our results to the data, as unbinned multivariate goodness-of-fit tests [19] have not yet gained much ground in the high-energy physics (HEP) sector.

5. Concluding Remarks

Let us present here very precisely the main conclusions of this work. Firstly, for these limited sets of data on production of soft particles in high-energy collisions which have, so far, defied explanation, we have attempted to provide two alternative theoretical/phenomenological approaches for their interpretation in modestly successful manners. Secondly, in fact, these two approaches conceptually and inwardly are somewhat interlinked, for which limited successes of both of them are not very surprising. Thirdly, the power-law models are seen to act much better here than all other models; besides, they are much more general than the others. Fourthly, the applications of power-law models are quite widespread in different fields of physics in particular and of science in general, for which active interests in investigating the origin of these power laws have been aroused. And this has, so far, given rise in the main, to two parallel streams of thought, of which one is the cascadisation phenomena and fractal mechanisms, and the other is the science of nonequilibrium phenomena that are generally probed by applying the Tsallis entropy and Tsallis statistics [20]. Confirmation of such multiply educated guesses can be made only by further dedicated researches in these fields.

At last, in response to what we learn very precisely from this work, we submit the following few points: (i) Our unquestioned belief in and reliance on the Standard Model (SM) have, so far, been virtually 'regimented', for which we fail to think of any other avenues and accept the singularity and uniqueness phenomena of the SM as taken for granted. (ii) In the sphere of surely very limited sets of data, we explore and assess here the potential of two alternative models in explaining the observed data. (iii) And as we have, in our opinion, succeeded in our attempts to

a considerable extent, these two models dealt herewith could in future be viewed and projected as possible alternative approaches to explain the nature of observed and measured data-sets on 'soft' production of particles in high-energy collisions.

Acknowledgements

The authors express their deep indebtedness to the learned referees for some encouraging remarks, constructive comments and valuable suggestions which helped a lot in improving an earlier version of the manuscript.

References

[1] Sunil Mukhi and Probir Roy, Pramana **73** (2009) 3.

[2] Wit Busza, Nucl. Phys. A **830** (2009) 35c.

[3] B. B. Back, Phys. Rev. C **72** (2005) 064906 [nucl-ex/0508018 v1 15 August 2005].

[4] B. De, S. Bhattacharyya and P. Guptaroy, J. Phys. G **28** (2002) 2963.

[5] B. De and S. Bhattacharyya, Int. J. Mod. Phys. A **19** (2004) 3225.

[6] B. De and S. Bhattacharyya, Mod. Phys. Lett. A **18** (2003) 1383.

[7] B. De and S. Bhattacharyya, Eur. Phys. J. A **19** (2004) 237.

[8] UA1 Collaboration (G. Arnison et al.), Phys. Lett. B **118** (1982) 167.

[9] UA1 Collaboration (G. Bocqet et al.), Phys. Lett. B **366** (1996) 434.

[10] WA80 Collaboration (R. Albrecht et al.), Eur. Phys. J. C **5** (1998) 255.

[11] R. Hagedorn, Riv. Nuovo Cimento **6** (1983) 46; R.Hagedorn, CERN-TH.3684 (1983).

[12] T. Peitzmann, Phys. Lett. B **450** (1999) 7.

[13] BRAHMS Collaboration (I. Arsene et al.), Phys. Rev. Lett. **91** (2003) 072305.

[14] G. Sau, S. K. Biswas, A. C. Das Ghosh, A. Bhattachrya and S. Bhattacharyya, Il Nuovo Cimento B **125** (2010) 833.

[15] S. Lehmann, A. D. Jackson and B. E. Lantrap, Physics/0512238 v1 24 December 2005.

[16] Ina Sarcevic, *Proc. Large Hadron Collidier Workshop*, vol. II, ed. by G. Jarlskog and D. Rein, CERN 90-10, ECFA 10-133(03 December 1990) 1214-1223.

[17] T. S. Biro and G. Purcsel, Phys. Rev. Lett **95** (2005) 162302.

[18] S. K. Biswas, G. Sau, B. De, A. Bhattacharya and S. Bhattacharyya, Hadronic J. **30** (2007) 533.

[19] Mike Williams, hep-ex/1006.3019 v1 15 June 2010.

[20] C. Tsallis, J. Stat. Phys. **52** (1988) 479; Physica A **221** (1995) 277; Braz. J. Phys. **29** (1999) 1; D. Prato and C. Tsallis, Phys. Rev. E **60** (1999) 2398.

[21] NA49 Collaboration (C. Alt et al.), Phys. Rev. C **77** (2008) 024903 [nucl-ex/0710.0118 v1 30 September 2007].

[22] NA49 Collaboration (C. Alt et al.), Phys. Rev. C **77** (2008) 064908 [nucl-ex/0709.4507 v2 26 September 2007].

[23] NA49 Collaboration (C. Alt et al.), Phys. Rev. C **77** (2008) 034906 [nucl-ex/0711.0547 v2 28 March 2008].

[24] STAR Collaboration (D. Cebra), nucl-ex/0903.4702 v1 (Submitted on 26 March 2009).

[25] Roppon Picha, Ph. D. Thesis, University of California, Davis, USA (2005).

TVORBA 'MEKIH' ČESTICA U Au+Au I Pb+Pb SUDARIMA NA VISOKIM ENERGIJAMA

Tvorba hadrona s malim p_T ('mekih') u sudarima na visokim energijama čini važan problem i od posebnog je zanimanja budući da teorija smetnje kvantne kromodinamike u tom području nije uspješna. U ovom smo radu istražili prirodu tvorbe lakih čestica u dvama simetričnim nuklearnim sudarima na dvije bliske energije i primjenom dvaju nestandardnih modela. Ishodi računa su u dobrom skladu s podacima. Usprkos tome, ostaju fenomenološke granice i ograničenja koje se ne mogu popraviti jer primijenjeni modeli ne daju dublje razumijevanje u fizičke procese u takvim sudarima.